

Numerical modeling of shock initiation in PETN by unified EOS

Shiro Kubota^{*†}, Tei Saburi^{*}, Yuji Ogata^{*}, and Kunihiro Nagayama^{**}

^{*}Research Core for Explosion Safety, Research Institute Science for safety and Sustainability, National Institute of Advanced Industrial Science and Technology, 16-1 Onogawa, Tsukuba, Ibaraki, 305-8569 JAPAN
TEL +81-29-861-8138 FAX +81-29-861-8138

[†]Corresponding address : kubota.46@aist.go.jp

^{**}Department of Aeronautics and Astronautics, Faculty of Engineering, Kyushu University, Fukuoka, 819-0395, JAPAN
TEL +81-92-802-3014 FAX +81-92-802-3017
E-mail : nagayama@aero.kyushu-u.ac.jp

Received : February 12, 2010 Accepted : March 16, 2010

Abstract

The numerical simulations of shock initiation of PETN were conducted using unified-form equations of state for reactant and detonation products phases. In our proposed modeling, the partially reacted state of PETN for arbitrary initial density can be calculated using only one parameter set in the case of theoretical maximum density. The equation of state for detonation products, which employs Grüneisen Γ as a function of the specific volume, and the Grüneisen equation of state with porous Hugoniot model as reference line for the reactant were used. The published shock initiation data were used to obtain the parameter for the initiation model. Finally we found the relationship between one parameter for the initiation model and the initial density.

Keywords : unified EOS, grüneisen EOS, porous hugoniot model, shock initiation, PETN

1. Introduction

Understanding of the initiation phenomena on high-energetic materials caused by external shock loading is important from the viewpoint of the safety engineering. The concept of the initiation is different between homogeneous and heterogeneous high-energetic materials¹⁻³⁾. The subject of this study is the initiation of the heterogeneous materials, such as a conventional solid explosive. When the shock wave enters the heterogeneous energetic materials, the local high-temperature and high-pressure regions that are created by shock interaction at the density discontinuity generate and trigger the subsequent reaction growth to attain the self-sustained rapid reaction⁴⁻⁶⁾. Because the partially reacted state for energetic materials is often treated as a simple mixture phase between the inert reactant and detonation product⁷⁻⁸⁾, the numerical simulation of the shock initiation requires a reaction rate model and equations of state (EOSs) for both phases. Even if the energetic materials are composed of identical constituents, the parameters have to be constructed for each initial density.

Moreover, the parameters of the EOSs for both phases are dependent on the initial density.

We propose the numerical modeling of the shock initiation by unified EOSs for both phases. The parameters of EOS for both phases are independent of the initial density. The proposed EOS for detonation products⁹⁻¹¹⁾ has been used for this study. For the inert reactant, the Grüneisen EOS with porous Hugoniot model^{12,13)} has been employed. The purpose of this study is to investigate the effect of the initial density of energetic material for the initiation phenomena, and to construct a unified initiation model. Because various published data including the initiation properties of PETN are available¹⁴⁻¹⁹⁾, PETN is selected as the subject of this numerical study.

2. Unified equations of state for detonation products and reactant phases

The EOS of detonation products⁹⁾ for PETN is the Grüneisen form with JWL²⁰⁻²²⁾ isentrope as a reference line, and is expressed as

$$P = \frac{\Gamma(v)}{v} (\varepsilon - \varepsilon_i^{TMD}) + P_i^{TMD} \quad (1)$$

$\Gamma(v)$ is the Grüneisen coefficient as a function of specific volume v . P and ε are the pressure and internal specific energy, respectively. The index TMD corresponds to the theoretical maximum density, the subscript i is the isentrope line that passes through the C-J point of the TMD case of PETN, and are expressed as

$$P_i^{TMD} = A \exp(-R_1 V) + B \exp(-R_2 V) + CV^{-(\omega+1)} \quad (2)$$

$$\varepsilon_i^{TMD} = -\int P_i^{TMD} dv \quad (3)$$

V is the ratio of the specific volume of the detonation products to that of the initial energetic material, and the parameters A, B, C, R_1, R_2 , and ω are constants.

For the unreacted reactant phase of PETN, the porous Hugoniot model was used and was combined with Grüneisen EOS. The shock compression curve for porous materials can be expressed using Hugoniot for the TMD case,

$$P_H^P = P_H^{TMD} \frac{K - v_0^{TMD}/v}{K - v_0^p/v} \quad (4)$$

where the subscript H represents the Hugoniot state, and the index p indicates the porous material. K is $2/\Gamma_s^{TMD} + 1$, and 0 corresponds to the initial state.

Specific volume and internal energy are assumed as the linear combination of two phases,

$$v = \lambda v_g + (1 - \lambda) v_s \quad (5)$$

$$\varepsilon = \lambda \varepsilon_g + (1 - \lambda) \varepsilon_s \quad (6)$$

and the pressure equilibrium condition, $P = P_s = P_g$, was assumed to determine the partially reacted state⁸⁾. The subscript s and g correspond to solid reactant and gaseous detonation product, respectively. λ is the mass fraction of detonation products estimated from the reaction rate law; $\lambda = 0$ corresponds to the unreacted state and $\lambda = 1$ to the completely reacted state. By using the above-mentioned EOS models for the detonation products and the reactant phases, only the parameter set for the TMD case of PETN is needed to compute the shock initiation of PETN for arbitrary initial density. Because an initial density of $1.77 \text{ g}\cdot\text{cm}^{-3}$ is very close to TMD for PETN, we regard this density as the TMD in this numerical study. The JWL parameter for PETN was referred from ref. (22). For the reactant phase, $U_s = 2.42 + 1.91Up$ and $\Gamma_u = 1.15$ were used¹⁶⁾.

3. Reaction rate model and numerical procedure

For the reaction rate model, the ignition and growth model²³⁾²⁴⁾ was used, which is expressed as

$$\frac{d\lambda}{dt} = I(1 - \lambda)^{2/9} \eta^4 + G(1 - \lambda)^{2/9} \lambda^{2/3} P^z \quad (7)$$

where $\eta = v_0/v - 1$. The parameters z, G , and I depend on the explosive properties and are adjusted on the basis of experimental data²⁴⁾. The subscript 0 indicates the initial state of a solid explosive. The first term of Eq.7 applies

from $\lambda = 0$ to the ignition term limit (IGL).

The governing equations are the one-dimensional mass, momentum, and energy conservation laws, which are solved by the finite difference method^{8),25)}. Impact problems of PETN and PMMA were solved with various initial densities. The initial mesh size of this simulation was set $50 \mu\text{m}$. The strategy of this numerical study is as follows. First, the parameters for the initiation model of the $1.72 \text{ g}\cdot\text{cm}^{-3}$ density case will be determined. As for the decided parameter, whether the result of an arbitrary initial density can be reproduced is examined. Since the reaction rate depends on the initial density, i. e., heterogeneities, the parameters may not be applicable to low-initial-density cases. However, the relation of the initial density and value of the parameters may be clarified. The first term in Eq.7 simulates the process of the hot spot formation, subsequent aggregation, and small reaction. In this simulation, we pay attention to growth process. It is reasonable to consider that the main reaction growth is expressed using the second term, and it depends on the initial density. The main parameters in the second term of Eq.7 are G and z . We select the exponent z as the subject of this numerical study. Except for z and IGL, all the parameters have been fixed.

4. Results and discussion

The relationship between the input pressure in PETN and the run distance to detonation is shown in Fig. 1. This relationship has been called the pop plot²⁶⁾. The solid symbols and + symbol were obtained using the parameters in Table. 1. In those cases, because the parameters were adjusted basis of the $1.72 \text{ g}\cdot\text{cm}^{-3}$ PETN, the good agreement between the published experimental data¹⁵⁾ and this numerical result can be confirmed. On the other hand, in the 1.6 and $1.4 \text{ g}\cdot\text{cm}^{-3}$ cases, a discrepancy can be observed. However, the slopes of the pop plot for the three initial densities were almost the same. The reaction rate increases with the exponent z decreases, therefore, when the exponent z is decreased, the run distance to detonation as the calculation result is decreased. The exponent z for 1.6 and $1.4 \text{ g}\cdot\text{cm}^{-3}$ was adjusted using trial and error simulations, so the simulation reproduced the published data as indicated by symbols \circ and \triangle in Fig. 1. Although the run distance to detonation decreases compared with that in the case of $z = 2.3$, the slopes of the pop plots for these density cases are almost the same as that in the case of $z = 2.3$.

The pop plot does not directly include information on the shock velocity. To check the velocity of the shock front in PETN, the relation between the time of the run distance and the run distance to detonation is also compared with the published data¹⁵⁾ and simulation results. The simulation results agree with the published data, as shown in Fig. 2. The above results indicate that this numerical simulation reproduces the published experimental data, such as the results of the wedge test.

Figure 3 shows the shock locus in PETN. To confirm the effect of the reaction on the propagation velocity of the shock front, the simulation result without reaction is also

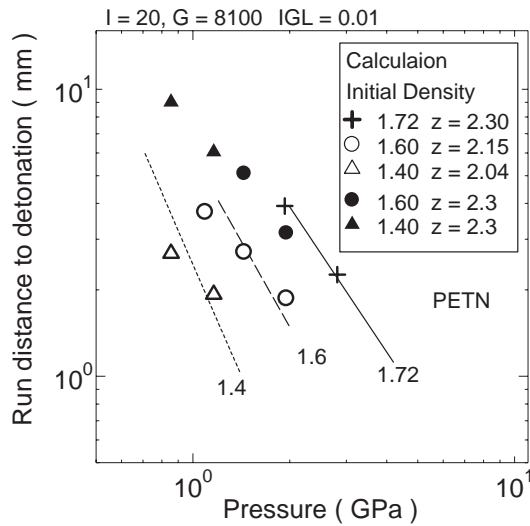


Fig. 1 Pressure vs. run distance to detonation (Pop plot) for PETN; The solid and dashed lines are the fitted line from a paper written by Stirpe, Johnson, and Wackerle¹⁵, and the dotted line from Cooper's paper²⁷.

Table 1 The parameters for ignition and growth model for PETN. The parameters were adjusted based on the 1.72 g·cm⁻³ initial density.

I (μsec ⁻¹)	G (μsec ⁻¹ Mbar ⁻¹)	z	IGL
20	8100	2.3	0.01

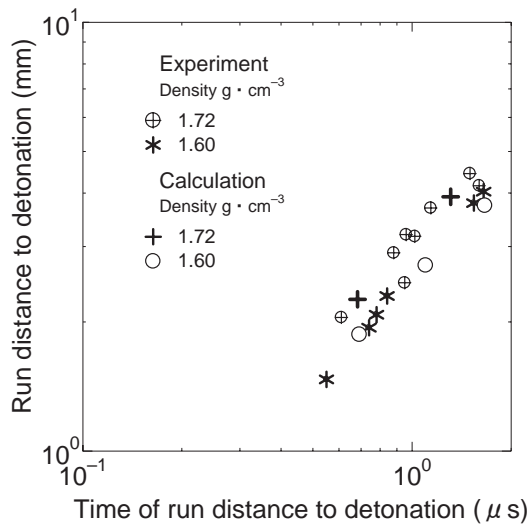
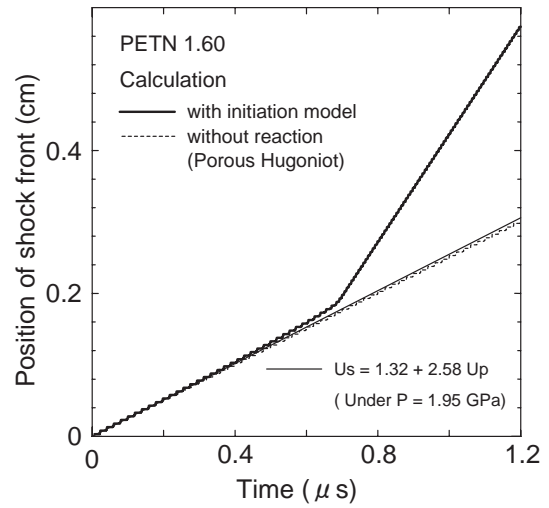
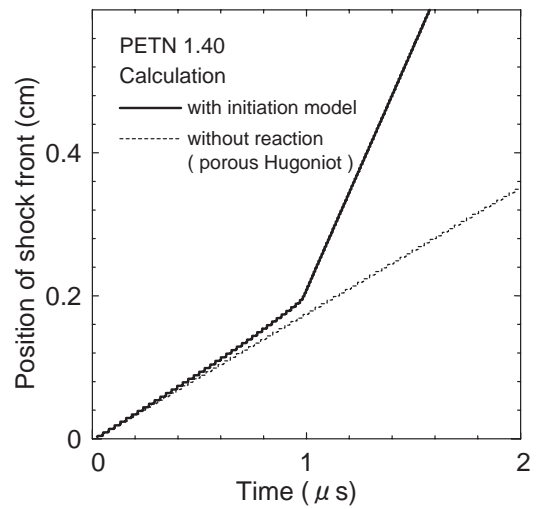


Fig. 2 The relation between the time of run distance and the run distance to detonation for PETN with 1.72 and 1.6 g·cm⁻³ initial density; Experimental data from a paper written by Stirpe, Johnson, and Wackerle¹⁵.

indicated by a dotted line. In Fig. 3 (a), the locus estimated by Hugoniot ($U_s = 1.32 + 2.58Up$)¹⁵ is also plotted. Two shock loci without reaction agree well, and this means that the porous Hugoniot model is appropriate for the reactant phase equation of state. The inflection point of the shock locus indicates the shock-to-detonation transition (SDT) point, and the numerical results indicates that the shock front is accelerated by the reaction wave just before the shock wave reaches the transition point. The difference between the SDT point and shock locus without reaction in the case of 1.4 g·cm⁻³ is



(a) 1.6 g·cm⁻³ initial density, sustained shock pulse 1.95 GPa.



(b) 1.4 g·cm⁻³ initial density, sustained shock pulse 1.44 GPa

Fig. 3 The shock locus in PETN; U_s ; shock velocity (km·s⁻¹), Up ; particle velocity (km·s⁻¹) $U_s - Up$ relation from a paper written by Stirpe, Johnson, and Wackerle¹⁵.

larger than that in the case of 1.6 g·cm⁻³. This result suggests that the shock front of the low density case is affected than that of the high density case.

The weak point of the porous Hugoniot model is that the model ignores the increase in pressure caused by the density change from the initial density to the theoretical maximum density. This weak point gave the inference of the calculation of the partially reacted state for the low-initial-density case. In the case of 1.0 g·cm⁻³ initial density, the shock velocity estimated by numerical simulation with the reaction model was markedly smaller than that without the initiation model. To avoid this situation, the IGL was adjusted in the case of 1.0 g·cm⁻³ initial density. From the theoretical maximum density to 1.4 g·cm⁻³ initial density, the IGL was set 0.01, so the ignition term did not have an effect on the velocity of the shock front before the SDT point.

Figure 4 shows the effect of the IGL on the velocity of the shock front in PETN 1.0 g·cm⁻³ initial density. The shock loci were obtained by the numerical simulation without a growth term. In the case of the IGL = 0.22, the veloc-

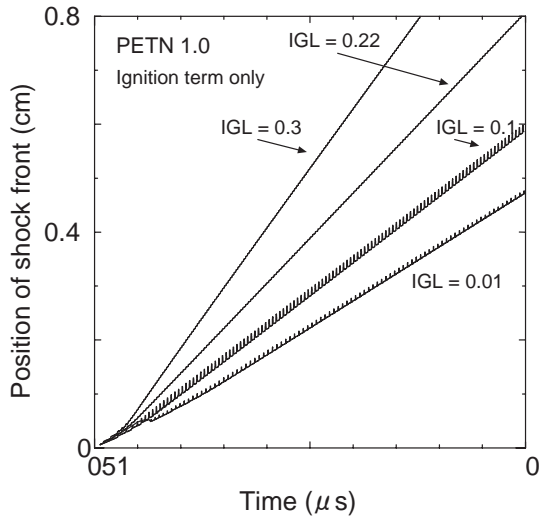


Fig. 4 The effect of the ignition limit (IGL) into the velocity of the shock front in PETN (The shock loci obtained by the numerical simulation without growth term).

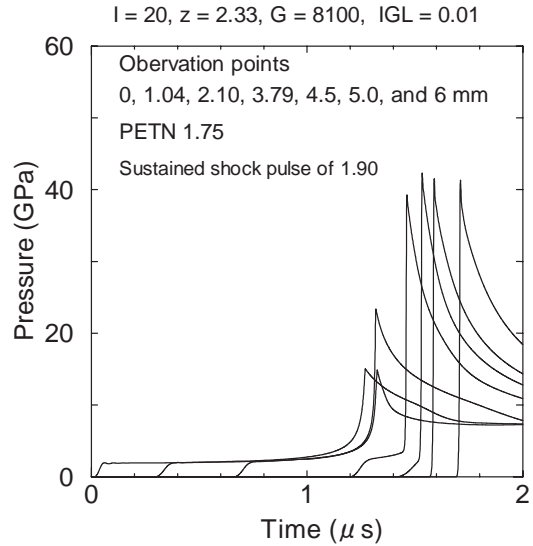


Fig. 7 The calculated pressure history in PETN with 1.75 g·cm⁻³ initial density.

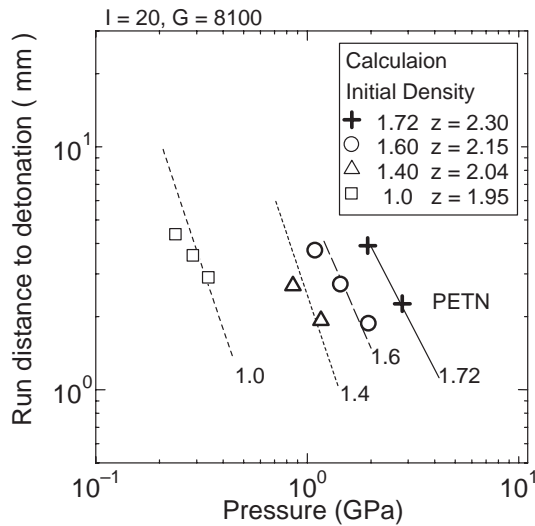


Fig. 5 Pop plot for PETN; The solid and dashed lines are the fitted line from a paper written by Stirpe, Johnson, and Wackerle¹⁵, and the two dotted lines from Cooper's paper²⁷.

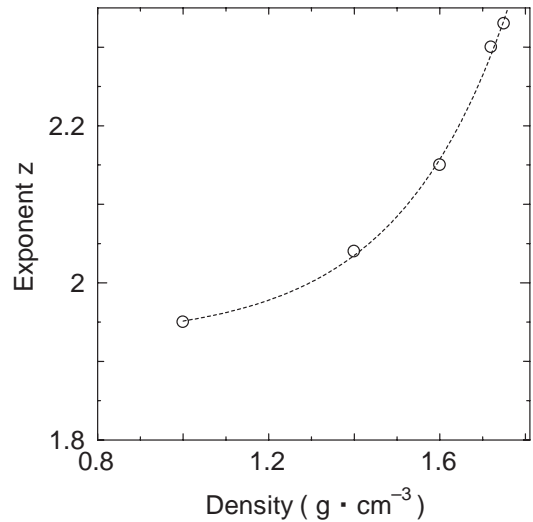


Fig. 8 The relationship between the initial density of PETN and the exponent z for initiation model; parameter z was estimated in this numerical study.

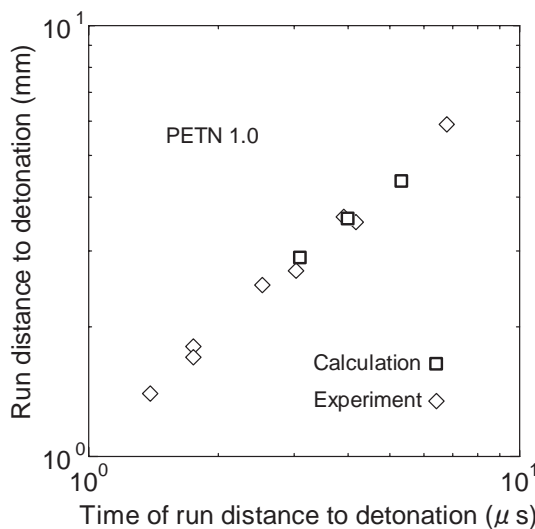


Fig. 6 The relationship between the time of run distance and the run distance to detonation for PETN with 1.0 g·cm⁻³ initial density; Experimental data from a paper written by Seay and Seely¹⁴.

ity of the shock front agrees with that obtained using the porous Hugoniot without a reaction. By using this IGL value, the exponent z was estimated by the simulation. The results of the 1.0 g·cm⁻³ initial density are plotted in Figs. 5 and 6 with square symbols. The simulation results simultaneously satisfy the pop plot²⁷ and the velocity information of the shock front¹⁴.

Figure 7 shows the pressure histories in PETN at various points obtained by numerical simulation of 1.75 g·cm⁻³ initial density. It is confirmed that these results indicate the good agreement with published pressure records¹⁹ and its numerical simulation by Lee and Tarver²³. In this case the 5 mm of run distance to detonation was reported, and our simulation represents the experimental results.

Figure 8 shows the relationship between the initial density of PETN and the exponent z in Eq.7. To be able to apply this simple modeling of the shock initiation phenomena for PETN for arbitrary initial density, this relation between the z and initial density is approximated using a function, $z = a + b \exp(\rho_0/c)$, where $a = 1.928$, $b = 5.056 \times$

10^{-4} , and $c = 0.26158$.

5. Conclusion

The numerical modeling of the shock initiation of PETN in this paper may be the first approach in this area as far as authors know. Although the widely used initiation model was employed, the feature of this approach was that the unified EOSs for the reactant and detonation products, which are independent of the initial density of PETN, were used for calculating the arbitrary initial density of PETN. It becomes possible to examine the initiation problem by our approach under a consistent concept although the concepts of the equations of state exist. In this paper, we focus on only one parameter of the initiation model. Finally, we found the relationship between one parameter and the initial density. This relation may be appropriate from $1.0 \text{ g}\cdot\text{cm}^{-3}$ initial density to the theoretical maximum density of PETN. Although an important engineering model was constructed in this paper, we would like to use this approach to understand the initiation phenomena in heterogeneous high-energetic materials.

References

- 1) A. N. Dremin, "Toward detonation theory", (1999) Springer-Verlag New York, Inc.
- 2) A. W. Campbell, C. W. Davis, and J. R. Travis, *Phys. Fluids* 4, 498 (1961).
- 3) A. W. Campbell, C. W. Davis, J. B. Ramsay, and J. R. Travis, *Phys. Fluids* 4, 511 (1961).
- 4) H. Eyring, R. E. Powell, G. H. Duffey, and R. B. Parlin, *Chem. Rev.* 45, 69 (1945).
- 5) C. L. Mader, *Phys. Fluids*, 8, 1811 (1965).
- 6) C. L. Mader, "An empirical model of heterogeneous shock initiation of the explosive 9404", Report No. LA-4475, Los Alamos Laboratory, (1970).
- 7) F. J. Petrone, *Phys. Fluids* 11, 1473 (1968).
- 8) S. Kubota, K. Nagayama, T. Saburi, and Y. Ogata, *Combust. Flame*, 151, 74 (2007).
- 9) K. Nagayama and S. Kubota, *J. Appl. Phys.*, 93, 2583 (2003).
- 10) K. Nagayama and S. Kubota, *Propellants, Explosives, Pyrotechnics*, 29, 118 (2004).
- 11) S. Kubota, T. Saburi, Y. Ogata, and K. Nagayama, *Sci. and Tech. Energetic Materials*, 71, 44 (2010).
- 12) Y. B. Zel'dovich and Y. P. Raizer, "Physics of Shock Waves and High-Temperature Hydrodynamic Phenomena", (2002), Dover Publications.
- 13) K. Nagayama and S. Kubota, *Proc. EuroPyro 2007, 34th International Pyrotechnics Seminar*, pp. 105-110 (2007), Beaune, France.
- 14) G. E. Seay and L. B. Seely, *J. Appl. Phys* 32, 1092 (1961).
- 15) D. Stirpe, J. O. Johnson, and J. Wackerle, *J. Appl. Phys.*, 41, 3884 (1970).
- 16) B. M. Dobratz, "LLNL Explosives Handbook, Properties of Chemical Explosives and Explosive Simulants", DE85-015961, UCRL-52997, UC-45, (1981) Univ. Calif., Livermore, California.
- 17) T. R. Gibbs and A. Popolato, "LASL explosive property data", (1980), University of California press.
- 18) J. J. Dick, *J. Appl. Phys* 81, 601 (1997).
- 19) J. Wackerle, J. O. Johnson, and P. M. Halleck, *Proc. Sixth Symposium (International) on Detonation*, pp. 20-28 (1976), Office of Naval Research-Department of the Navy, Coronado, CA.
- 20) E. L. Lee, H. C. Hornig and J. W. Kury, "Adiabatic expansion of high explosive detonation products", Report No. UCRL-50422, Lawrence Radiation Laboratory, (1968).
- 21) J. W. Kury, H. C. Hornig, E. L. Lee, J. L. McDonnell, D. L. Ornellas, M. Finger, F. M. Strange, and M. L. Wilkins, *Proc. 4th Symposium (International) on Detonation*, pp. 3-13 (1965), Naval Ordnance Laboratory ACR-126, Washington, DC.
- 22) E. Lee, M. Finger, and W. Collins, "JWL equation of state coefficients for high explosive" LLNL report, UCID-16189 (1973).
- 23) E. L. Lee C. M. Tarver, *Phys. Fluids* 23, 2362 (1980).
- 24) C. M. Tarver, J. O. Hallquist, and L. M. Erickson, *Proc. Eighth Symposium (International) on Detonation*, pp. 951-961 (1985), Naval Surface Weapons Center NSWC 86-194, Albuquerque, NM.
- 25) C. L. Mader, "Numerical Modeling of Detonations", (1979), University of California Press.
- 26) J. B. Ramsay and A. Popolato, *Proc. Fourth Symposium (International) on Detonation*, pp. 233-238 (1965) Naval Ordnance Laboratory ACR-126, Washington, DC.
- 27) P. W. Cooper, *Proc. Tenth Symposium (International) on Detonation*, pp. 690-695 (1993), Office of Naval Research ONR 33395-12, Boston, MA.

統合状態方程式を用いたPETNの衝撃起爆過程のモデリング

久保田士郎*[†], 佐分利禎*, 緒方雄二*, 永山邦仁**

固体ならびに爆轟ガス成分の統合形式状態方程式を用いてPETNの衝撃起爆過程の数値計算を実施した。我々の提案するモデルリングでは、任意の初期密度のPETNに対して、反応途中の状態は理論密度のパラメータセットだけを用いて計算できる。爆轟生成ガス成分には、比体積の関数として表せるグリユナイゼン Γ を用いた状態式を、固体成分には多孔質体ウゴニオモデルを参照線とするグリユナイゼン状態方程式を用いた。公表された衝撃起爆データを用いて起爆モデルのパラメータを求めた。その結果、初期密度と起爆モデルパラメータの関係が求められた。

*独立行政法人産業技術総合研究所安全科学研究部門爆発安全研究コア

〒305-8569 つくば市小野川16-1

[†]Corresponding address: kubota.46@aist.go.jp

**九州大学大学院工学研究院航空宇宙工学部門 〒819-0359 福岡市西区元岡774